

Time Delay Estimation for Sinusoidal Signals

H. C. So

Department of Electronic Engineering, The Chinese University of Hong Kong
Shatin, N.T., Hong Kong

SP EDICS: 1-DETC

January 25, 2000

Abstract

The problem of estimating the difference in arrival times of a sinusoid received at two spatially separated sensors is considered. Given the sinusoidal frequency, a simple delay estimator using the phase difference of the discrete time Fourier transforms (DTFTs) of the received signals is devised. With the use of periodogram, the algorithm is extended to estimate the delay when the frequency is unknown. The minimum achievable delay variances for the cases of known/unknown frequencies and constant/rectangular envelopes are also derived. The effectiveness of the method is demonstrated by comparing with the performance bounds for different frequencies, envelopes and noise conditions.

Contact Information:

H. C. So

Department of Electronic Engineering

The Chinese University of Hong Kong

Shatin, N.T., Hong Kong

Tel : (852) 2609 8456

Fax: (852) 2603 5558

email: hcs0@ee.cuhk.edu.hk

I. Introduction

Estimation of the time delay between two noisy versions of the same signal received at two spatially separated sensors has important applications such as direction finding, source localization and velocity tracking [1]. The mathematical model of the discrete-time sensor outputs is given by

$$r_1(n) = s(n) + q_1(n) \tag{1}$$

$$r_2(n) = s(n - D) + q_2(n), \quad n = 0, 1, \dots, N - 1$$

where $s(n)$ is the signal of interest, $q_1(n)$ and $q_2(n)$ represent additive noises which are independent of $s(n)$, D is the difference in arrival times at the two receivers and N is the number of samples collected at each channel. Without loss of generality, the sampling interval is assigned to be unity second.

Many methods have been proposed for time delay estimation in the past two decades [1]-[8]. Generalized cross correlator (GCC) [2]-[4] is a conventional approach to the problem and its delay estimate is found by locating the peak of the cross correlation function of the filtered versions of $r_1(n)$ and $r_2(n)$. When $s(n)$, $q_1(n)$ and $q_2(n)$ are all uncorrelated Gaussian variables, it has been proved [2] that the GCC can provide maximum likelihood (ML) delay estimation. However, implementation of the GCC requires *a priori* statistics of the received signals and thus in the absence of these information, the desired performance is difficult to achieve in practice [4]. Moreover, it fails to work if the noises are impulsive [5] or spatially correlated [7]. In the presence of impulsive noise modeled as alpha-stable random process, accurate delay estimates can be attained using the fractional lower order statistics (FLOS) based techniques [5]-[6]. On the other hand, the higher order statistics (HOS) approach is an effective solution for correlated noises when the signal is a non-Gaussian random process and the noises are Gaussian distributed [7] or vice versa [8].

The aim of this paper is to devise a simple and accurate time delay estimator when the source signal is deterministic, specifically for a pure sinusoid that commonly occurs in radar, sonar and digital communications [9]-[11], although the GCC can be employed in deterministic signal condition [3]. In our study, we consider that $s(n)$ is analytic and has the form

$$s(n) = a(n) \exp(j\omega_0 n + \phi) \tag{2}$$

where $a(n)$, $\omega_0 \in (0, \pi)$ and $\phi \in [0, 2\pi)$ represent the real envelope function, radian frequency and unknown constant phase of the sinusoid, respectively. It is assumed that $q_1(n)$ and $q_2(n)$ are uncorrelated zero-mean complex white Gaussian processes with variance σ_q^2 and $D \in (-\pi/\omega_0, \pi/\omega_0)$ to avoid ambiguous delay estimates.

The paper is organized as follows. Based on the discrete-time Fourier transforms (DTFTs) [12] of the two sensor outputs, a computationally efficient delay estimation algorithm for sinusoidal signals is developed in Section II, assuming that ω_0 is known. The estimator variance in the case of constant

envelope is also derived. Section III modifies the proposed method for unknown frequency with the use of periodogram. The Cramér-Rao lower bounds (CRLBs) [10] of the delay estimates for the cases of known/unknown frequencies and constant/rectangular envelopes are derived in Section IV. Section V evaluates the estimation accuracy of the DTFT based approach via comparison with the performance bounds, and finally, conclusions are drawn in Section VI.

II. The Proposed Method

In this section, a simple delay estimator for sinusoidal signals with known frequency is developed. For ease of analysis, we assume that the signal has an unknown constant envelope with $a(n) = A$, $n = 0, 1, \dots, N - 1$, although the proposed method can work for other envelopes. The DTFT of $r_1(n)$ is given by

$$\begin{aligned} R_1(\omega) &= \sum_{n=0}^{N-1} r_1(n) e^{-j\omega n} \\ &= A e^{j(\phi + (\omega_0 - \omega)(N-1)/2)} \frac{\sin\left(\frac{(\omega_0 - \omega)N}{2}\right)}{\sin\left(\frac{\omega_0 - \omega}{2}\right)} + \sum_{n=0}^{N-1} q_1(n) e^{-j\omega n} \end{aligned} \quad (3)$$

In the time domain, the signal-to-noise ratio (SNR) of $r_1(n)$, denoted by SNR_1 , is equal to A^2/σ_q^2 . On the other hand, it can be easily shown from (3) that the SNR of $|R_1(\omega_0)|^2$, SNR_2 , has a value of NA^2/σ_q^2 , which is N times larger than SNR_1 . It is because the signal power is concentrated at $\omega = \omega_0$ while the noise power equals $N\sigma_q^2$ for all frequencies in the DTFT domain. Motivated by this fact, the DTFTs of the sensor outputs at $\omega = \omega_0$ are used to estimate the time delay as follows. For $\text{SNR}_1 \gg 1$, $R_1(\omega_0)$ can be approximated as [13]

$$\begin{aligned} R_1(\omega_0) &= NAe^{j\phi} + \sum_{n=0}^{N-1} q_1(n) e^{-j\omega_0 n} \\ &\approx NAe^{j\phi} e^{j\Im\{X(\omega_0)\}} \end{aligned} \quad (4)$$

where

$$X(\omega_0) = \frac{1}{NA} \sum_{n=0}^{N-1} q_1(n) e^{-j(\omega_0 n + \phi)} \quad (5)$$

and $\Im\{x\}$ denotes the imaginary part of x . The phase angle of $R_1(\omega_0)$ is thus of the form

$$\angle\{R_1(\omega_0)\} \approx \phi + \Im\{X(\omega_0)\} \quad (6)$$

whose mean value is ϕ and has a variance of $1/(2\text{SNR}_2)$. Similarly, the phase of the DTFT of $r_2(n)$ at $\omega = \omega_0$ is given by

$$\angle\{R_2(\omega_0)\} \approx \phi - \omega_0 D + \Im\{Y(\omega_0)\} \quad (7)$$

where

$$Y(\omega_0) = \frac{1}{NA} \sum_{n=0}^{N-1} q_2(n) e^{-j(\omega_0(n-D)+\phi)} \quad (8)$$

The quantity $\angle\{R_2(\omega_0)\}$ has the expected value of $\phi - \omega_0 D$ and its variance is identical to that of $\angle\{R_1(\omega_0)\}$.

Using the phase difference of $R_1(\omega_0)$ and $R_2(\omega_0)$, the delay estimate, denoted by \hat{D} , is computed as

$$\hat{D} = \frac{\angle\{R_1(\omega_0)R_2^*(\omega_0)\}}{\omega_0} \quad (9)$$

where $*$ represents the conjugate operation.

Let $\gamma_1 = \Re\{\sum_{n=0}^{N-1} q_1(n)e^{-j\omega_0 n}\}$, $\gamma_2 = \Im\{\sum_{n=0}^{N-1} q_1(n)e^{-j\omega_0 n}\}$, $\gamma_3 = \Re\{\sum_{n=0}^{N-1} q_2(n)e^{-j\omega_0 n}\}$ and $\gamma_4 = \Im\{\sum_{n=0}^{N-1} q_2(n)e^{-j\omega_0 n}\}$ where $\Re\{x\}$ represents the real part of x . Notice that these four terms contribute to the random components of \hat{D} and they are independent to each other and have zero means. As a result, the variance of \hat{D} , denoted by $\text{var}(\hat{D})$, is fully due to the noise terms $\gamma_1, \gamma_2, \gamma_3$ and γ_4 and it is given by [14]

$$\text{var}(\hat{D}) = \sum_{i=1}^4 \left(\frac{\partial \hat{D}}{\partial \gamma_i} \Big|_{\gamma_i = E\{\gamma_i\}} \right)^2 E\{\gamma_i^2\} \quad (10)$$

where E is the expectation operation. This expression can be simplified and modified to (Appendix I)

$$\text{var}(\hat{D}) = \min \left\{ \frac{\pi^2}{3\omega_0^2}, \frac{1}{\omega_0^2 NSNR_1} \right\} \quad (11)$$

which is a constant if $NSNR_1 < 3/\pi^2$, and is inversely proportional to ω_0, N and SNR_1 , otherwise.

III. Extension to Unknown Frequency

It is well known that [15] the periodogram will give the ML estimate of frequency for a single complex sinusoid in white noise. With the use of periodogram, an iterative procedure is proposed to find D when ω_0 is not known, as follows.

1. Use periodogram to get an initial estimate of $\omega_0, \hat{\omega}_0$:

$$\hat{\omega}_0 = \frac{\arg \max_{\omega} \{P_{r_1}(\omega)\} + \arg \max_{\omega} \{P_{r_2}(\omega)\}}{2} \quad (12)$$

where

$$P_x(\omega) = \frac{1}{N} \left| \sum_{n=0}^{N-1} x(n) e^{-j\omega n} \right|^2 \quad (13)$$

denotes the periodogram of $x(n)$.

2. Compute the initial delay estimate as

$$\hat{D} = \frac{\angle\{R_1(\hat{\omega}_0)R_2^*(\hat{\omega}_0)\}}{\hat{\omega}_0} \quad (14)$$

3. Construct a $2N$ -length sequence $z(n)$ from $r_1(n)$ and $r_2(n)$ of the form

$$z(n) = \begin{cases} r_1(n) & , \quad n = 0, \dots, N-1 \\ r_2(n-N)e^{j\hat{\omega}_0(\hat{D}+N)} & , \quad n = N, \dots, 2N-1 \end{cases} \quad (15)$$

which can be considered as a noisy sinusoid with frequency ω_0 . Since the variance of the ML frequency estimate is asymptotically proportional to one over the cube of the observation length [15], $z(n)$ is employed to find a more accurate estimate of ω_0 :

$$\hat{\omega}_0 = \arg \max_{\omega} \{P_z(\omega)\} \quad (16)$$

4. Repeat steps 2 and 3 for a few times until convergence. In the simulation examples in Section V, at most five iterations are required for the parameters to converge.

The delay variance of the proposed method in the case of unknown frequency is derived as (Appendix II)

$$\text{var}(\hat{D}) = \min \left\{ \frac{\pi^2}{3\omega_0^2}, \frac{1}{\omega_0^2 N \text{SNR}_1} + \frac{3D^2}{\omega_0^2 N(N^2-1)\text{SNR}_1} \right\} \quad (17)$$

Notice that the difference between (17) and (11) is negligible particularly for sufficiently large N .

IV. Derivation of Performance Bounds

We first derive the CRLB of the delay estimate for known ω_0 . The key is to group ω_0 and D as one variable, say, $\theta = \omega_0 D$, and combine $r_1(n)$ and $r_2(n)$ to form a $2N$ -length sequence $\{w(n)\} = \{r_1(0), \dots, r_1(N-1), r_2(0), \dots, r_2(N-1)\}$. The probability density function (PDF) of $w(n)$ is given by [11]

$$p(w; \rho) = \frac{1}{\pi^{2N} \sigma_q^{4N}} \exp \left\{ -\frac{1}{\sigma_q^2} \left(\sum_{n=0}^{N-1} |r_1(n) - Ae^{j(\omega_0 n + \phi)}|^2 + \sum_{n=0}^{N-1} |r_2(n) - Ae^{j(\omega_0 n - \theta + \phi)}|^2 \right) \right\} \quad (18)$$

where $\rho = [A, \phi, \theta]$ is the unknown parameter vector to be estimated. The 3×3 Fisher information matrix has the form [10]

$$I(\rho) = \begin{bmatrix} -E \left[\frac{\partial^2 \ln p(w; \rho)}{\partial A^2} \right] & -E \left[\frac{\partial^2 \ln p(w; \rho)}{\partial A \partial \phi} \right] & -E \left[\frac{\partial^2 \ln p(w; \rho)}{\partial A \partial \theta} \right] \\ -E \left[\frac{\partial^2 \ln p(w; \rho)}{\partial \phi \partial A} \right] & -E \left[\frac{\partial^2 \ln p(w; \rho)}{\partial \phi^2} \right] & -E \left[\frac{\partial^2 \ln p(w; \rho)}{\partial \phi \partial \theta} \right] \\ -E \left[\frac{\partial^2 \ln p(w; \rho)}{\partial \theta \partial A} \right] & -E \left[\frac{\partial^2 \ln p(w; \rho)}{\partial \theta \partial \phi} \right] & -E \left[\frac{\partial^2 \ln p(w; \rho)}{\partial \theta^2} \right] \end{bmatrix} \quad (19)$$

It is clear that the matrix is symmetric since the order of partial differentiation can be interchanged. The log-likelihood function is

$$\begin{aligned} \ln p(w, \rho) = & -\ln(\pi^{2N} \sigma_q^{4N}) - \frac{1}{\sigma_q^2} \left[\sum_{n=0}^{N-1} (|r_1(n)|^2 + |r_2(n)|^2 + 2A^2 - r_1(n)Ae^{-j(\omega_0 n - \theta + \phi)} - \right. \\ & \left. r_1^*(n)Ae^{j(\omega_0 n + \phi)} - r_2(n)Ae^{-j(\omega_0 n - \theta + \phi)} - r_2^*(n)Ae^{j(\omega_0 n - \theta + \phi)}) \right] \end{aligned} \quad (20)$$

The derivatives are easily found as

$$E \left\{ \frac{\partial^2 \ln p(w, \rho)}{\partial A^2} \right\} = -\frac{4N}{\sigma_q^2} \quad (21)$$

$$E \left\{ \frac{\partial^2 \ln p(w, \rho)}{\partial \phi^2} \right\} = -\frac{4N A^2}{\sigma_q^2} \quad (22)$$

$$E \left\{ \frac{\partial^2 \ln p(w, \rho)}{\partial \theta^2} \right\} = -\frac{2N A^2}{\sigma_q^2} \quad (23)$$

$$E \left\{ \frac{\partial^2 \ln p(w, \rho)}{\partial \phi \partial \theta} \right\} = \frac{2N A^2}{\sigma_q^2} \quad (24)$$

$$E \left\{ \frac{\partial^2 \ln p(w, \rho)}{\partial A \partial \phi} \right\} = E \left\{ \frac{\partial^2 \ln p(w, \rho)}{\partial A \partial \theta} \right\} = 0 \quad (25)$$

The CRLB for θ , $\text{CRLB}(\theta)$, is obtained from the inverse of $I(\rho)$ [10] and has the expression

$$\text{CRLB}(\theta) = \frac{1}{N \text{SNR}_1} \quad (26)$$

Using [14] and (26), the CRLB for D , denoted by $\text{CRLB}(D)$, is evaluated as

$$\text{CRLB}(D) = \frac{1}{\omega_0^2 N \text{SNR}_1} \quad (27)$$

Assuming the delay is uniformly distributed between $-\pi/\omega_0$ and π/ω_0 , the composite bound for the delay is identical to (11) which means that the proposed method provides the optimal delay estimation performance for sinusoidal signals with known frequency and constant envelope.

In the case of unknown frequency, the parameter vector will become $\rho = [A, \phi, \theta, \omega_0]$ and the size of the corresponding Fisher information matrix is 4×4 . The following partial derivatives are needed and they are calculated straightforwardly as

$$E \left\{ \frac{\partial^2 \ln p(w, \rho)}{\partial \omega_0^2} \right\} = -\frac{2A^2 N(N-1)(2N-1)}{3\sigma_q^2} \quad (28)$$

$$E \left\{ \frac{\partial^2 \ln p(w, \rho)}{\partial \omega_0 \partial A} \right\} = 0 \quad (29)$$

$$E \left\{ \frac{\partial^2 \ln p(w, \rho)}{\partial \omega_0 \partial \phi} \right\} = -\frac{2A^2 N(N-1)}{\sigma_q^2} \quad (30)$$

$$E \left\{ \frac{\partial^2 \ln p(w, \rho)}{\partial \omega_0 \partial \theta} \right\} = -\frac{A^2 N(N-1)}{\sigma_q^2} \quad (31)$$

Using (21)-(25) and (28)-(31), the CRLBs for ω_0 and θ are computed as

$$\text{CRLB}(\omega_0) = \frac{3}{N(N^2 - 1)\text{SNR}_1} \quad (32)$$

and

$$\text{CRLB}(\theta) = \frac{1}{N\text{SNR}_1} \quad (33)$$

The CRLB for D is only dependent on $\text{CRLB}(\omega_0)$ and $\text{CRLB}(\theta)$ [14] and can be shown to be

$$\text{CRLB}(D) = \frac{1}{\omega_0^2 N \text{SNR}_1} + \frac{3D^2}{\omega_0^2 N (N^2 - 1) \text{SNR}_1} \quad (34)$$

As a result, the composite performance bound is identical to (17) and thus the proposed method also gives the minimum delay variance for the unknown frequency case.

When the source signal is a gated sinusoid, that is, $a(n) = A$ for $n = 0, 1, \dots, L - 1$ and equals 0 otherwise, it can be shown in a similar way that the performance bounds of the delay estimate are given by (11) and (17) for known and unknown ω_0 , respectively, with the substitution of $L = N$.

V. Simulation Results

Extensive computer simulations had been done to corroborate the theoretical derivations and to evaluate the performance of the proposed approach for estimating the time delay between sinusoidal signals. The mean square delay errors (MSFEs) for the cases of known/unknown frequencies and constant/rectangular envelopes were investigated. The tone parameters A and ϕ were assigned to be 1 and 0.1, respectively, while the time delay was set to 0.6s. Different SNR_1 s were produced by properly scaling the noise variance. Unless stated otherwise, the sinusoidal frequency ω_0 and the observation length N had values of 0.345π rad/s and 32, respectively. Five iterations of (14) and (16) were used when the value of ω_0 was not available. All simulation results provided were averages of 1000 independent runs.

Figure 1 shows the MSFEs of the proposed method for a constant envelope sinusoid with known frequency at different N versus SNR_1 . It is seen that except in the no information region, the MSFE decreased as the observation interval increased. Furthermore, the delay variances agreed with the theoretical values very well particularly for $\text{SNR}_1 \geq -5\text{dB}$ for all cases. The delay estimation performances using the sinusoidal signal at different known frequencies are compared in Figure 2. We observe that the MSFEs decreased as the frequency increased and they were close to the corresponding performance bounds. Figure 3 illustrates the MSFEs when the source signal was a gated sinusoid with different lengths of the rectangular envelope. As expected, the accuracy of \hat{D} increased with L . In addition, it can be seen that MSFEs were above the performance bounds by approximately 1.31dB and 3.27dB at $L = 0.75N$ and $L = 0.5N$ for $\text{SNR}_1 \geq -5\text{dB}$, respectively. This implies that the optimality of the proposed method will degrade as the width of the signal envelope decreases.

The variances of \hat{D} when $s(n)$ was a pure sinusoid with unknown ω_0 are plotted in Figure 4. It is observed that the proposed method met the performance bound and performed very similar to the known frequency case for $\text{SNR}_1 \geq -4\text{dB}$. Below the threshold SNR of -4dB , the MSFEs became much larger than the composite bound which was due to the occurrence of anomalous $\hat{\omega}_0$ in the nonlinear frequency estimation process [15]. The test of Figure 3 was repeated for unknown ω_0 and the results are shown in Figure 5. We see that the MSFEs were close to those of Figure 3 when the SNRs were greater than the threshold SNRs of -4dB , -3dB and -1dB for $L = N$, $L = 0.75N$ and $L = 0.5N$, respectively.

VI. Conclusions

An DTFT based method has been derived for estimating the time difference of arrival between sinusoidal signals received at two separated sensors. When the tone frequency is available, the delay estimate is given by the phase difference of the DTFTs of the received signals over the frequency. An iterative delay estimation procedure using the periodogram is also developed for the case of unknown frequency. It is proved that the variances of the delay estimates can meet the performance bounds for known and unknown frequencies when the sinusoid has a constant envelope. Numerical examples are included to validate the theoretical analysis and to demonstrate the effectiveness of the proposed approach.

Appendix I

The derivation of (11) is given as follows. First, the real and imaginary parts of $R_1(\omega_0)R_2^*(\omega_0)$ are of the forms

$$\begin{aligned} \Re\{R_1(\omega_0)R_2^*(\omega_0)\} &= N^2A^2 \cos(\omega_0D) + NA \cos(\phi)\gamma_3 + NA \cos(\phi - \omega_0D)\gamma_1 + NA \sin(\phi)\gamma_4 \\ &\quad + NA \sin(\phi - \omega_0D)\gamma_2 + \gamma_1\gamma_3 + \gamma_2\gamma_4 \end{aligned}$$

and

$$\begin{aligned} \Im\{R_1(\omega_0)R_2^*(\omega_0)\} &= N^2A^2 \sin(\omega_0D) - NA \cos(\phi)\gamma_4 - NA \sin(\phi - \omega_0D)\gamma_1 + NA \sin(\phi)\gamma_3 \\ &\quad + NA \cos(\phi - \omega_0D)\gamma_2 - \gamma_1\gamma_4 + \gamma_2\gamma_3 \end{aligned}$$

Let $\Psi = \Im\{R_1(\omega_0)R_2^*(\omega_0)\}/\Re\{R_1(\omega_0)R_2^*(\omega_0)\}$ and noting that $\angle\{R_1(\omega_0)R_2^*(\omega_0)\} = \tan^{-1}(\Psi)$, the partial derivative of \hat{D} with respect to γ_1 at $\gamma_i = E\{\gamma_i\} = 0$, $i = 1, 2, 3, 4$, is then computed as

$$\begin{aligned} \left. \frac{\partial \hat{D}}{\partial \gamma_1} \right|_{\gamma_i=0} &= \frac{1}{\omega_0} \cdot \left. \frac{\partial \tan^{-1}(\Psi)}{\partial \Psi} \right|_{\gamma_i=0} \cdot \left. \frac{\partial \Psi}{\partial \gamma_1} \right|_{\gamma_i=0} \\ &= \frac{1}{\omega_0} \cdot \frac{1}{1 + \tan^2(\omega_0D)} \end{aligned}$$

$$= \frac{N^2 A^2 \cos(\omega_0 D) \cdot -NA \sin(\phi - \omega_0 D) - N^2 A^2 \sin(\omega_0 D) \cdot NA \cos(\phi - \omega_0 D)}{(N^2 A^2 \cos(\omega_0 D))^2} = -\frac{\sin(\phi)}{NA\omega_0} \quad (\text{A.1})$$

Similarly, the partial derivative of \hat{D} with respect to γ_2 , γ_3 and γ_4 can be shown to be

$$\left. \frac{\partial \hat{D}}{\partial \gamma_2} \right|_{\gamma_i=0} = \frac{\cos(\phi)}{NA\omega_0} \quad (\text{A.2})$$

$$\left. \frac{\partial \hat{D}}{\partial \gamma_3} \right|_{\gamma_i=0} = \frac{\sin(\phi - \omega_0 D)}{NA\omega_0} \quad (\text{A.3})$$

and

$$\left. \frac{\partial \hat{D}}{\partial \gamma_4} \right|_{\gamma_i=0} = -\frac{\cos(\phi - \omega_0 D)}{NA\omega_0} \quad (\text{A.4})$$

From (A.1)-(A.4) and (10) with the use of $E\{\gamma_i^2\} = N\sigma_q^2/2$ for $i = 1, 2, 3, 4$, we have

$$\text{var}(\hat{D}) = \frac{1}{\omega_0 N \text{SNR}_1} \quad (\text{A.5})$$

Assuming that D is uniformly distributed in $(-\pi/\omega_0, \pi/\omega_0)$ and combining (A.5) yield the composite bound for the variance of \hat{D}

$$\text{var}(\hat{D}) = \min \left\{ \frac{\pi^2}{3\omega_0^2}, \frac{1}{\omega_0^2 N \text{SNR}_1} \right\}$$

which is (11).

Appendix II

The variance of \hat{D} for unknown ω_0 is derived as follows. Let the steady state frequency estimate of (16) be $\hat{\omega}_0 = \omega_0 + \gamma_5$ where γ_5 is the zero-mean estimation error of ω_0 and $f(\gamma_5) = \sin(\gamma_5(N-1)/2)/\sin(\gamma_5/2)$. It has been revealed that the variance of $\hat{\omega}_0$ or $E\{\gamma_5^2\}$ is equal to CRLB(ω_0) of (32). In this case, $\text{var}(\hat{D})$ is fully due to $\gamma_1, \gamma_2, \gamma_3, \gamma_4$ and γ_5 . Following Appendix I, the real and imaginary parts of $R_1(\hat{\omega}_0)R_2^*(\hat{\omega}_0)$ are evaluated as

$$\begin{aligned} \Re\{R_1(\hat{\omega}_0)R_2^*(\hat{\omega}_0)\} &= A^2 \cos(\omega_0 D) f^2(\gamma_5) + A \cos\left(\phi + \frac{\gamma_5(N-1)}{2}\right) f(\gamma_5) \gamma_3 \\ &+ A \cos\left(\phi - \omega_0 D + \frac{\gamma_5(N-1)}{2}\right) f(\gamma_5) \gamma_1 + A \sin\left(\phi + \frac{\gamma_5(N-1)}{2}\right) f(\gamma_5) \gamma_4 \\ &+ A \sin\left(\phi - \omega_0 D + \frac{\gamma_5(N-1)}{2}\right) f(\gamma_5) \gamma_2 + \gamma_1 \gamma_3 + \gamma_2 \gamma_4 \end{aligned}$$

and

$$\begin{aligned} \Im\{R_1(\hat{\omega}_0)R_2^*(\hat{\omega}_0)\} &= A^2 \sin(\omega_0 D) f^2(\gamma_5) - A \cos\left(\phi + \frac{\gamma_5(N-1)}{2}\right) f(\gamma_5) \gamma_4 \\ &- A \sin\left(\phi - \omega_0 D + \frac{\gamma_5(N-1)}{2}\right) f(\gamma_5) \gamma_1 + A \sin\left(\phi + \frac{\gamma_5(N-1)}{2}\right) f(\gamma_5) \gamma_3 \\ &+ A \cos\left(\phi - \omega_0 D + \frac{\gamma_5(N-1)}{2}\right) f(\gamma_5) \gamma_2 - \gamma_1 \gamma_4 + \gamma_2 \gamma_3 \end{aligned}$$

Denote $\hat{\Psi} = \Im\{R_1(\hat{\omega}_0)R_2^*(\hat{\omega}_0)\}/\Re\{R_1(\hat{\omega}_0)R_2^*(\hat{\omega}_0)\}$. It can be shown that the partial derivatives of \hat{D} with respect to $\gamma_1, \gamma_2, \gamma_3$ and γ_4 at $\gamma_i = 0$ for $i = 1, 2, \dots, 5$, are given by (A.1) to (A.4), respectively, while

$$\left. \frac{\partial \hat{D}}{\partial \gamma_5} \right|_{\gamma_i=0} = -\frac{D}{\omega_0} \quad (\text{A.6})$$

The variance of \hat{D} is then computed as

$$\begin{aligned} \text{var}(\hat{D}) &= \sum_{i=1}^5 \left(\left. \frac{\partial \hat{D}}{\partial \gamma_i} \right|_{\gamma_i=0} \right)^2 E\{\gamma_i^2\} \\ &= \frac{1}{\omega_0^2 N \text{SNR}_1} + \frac{3D^2}{\omega_0^2 N(N^2 - 1) \text{SNR}_1} \end{aligned}$$

Combining the results, we obtain the composite delay variance which is equal to (17), with the assumption that D is uniformly distributed in $(-\pi/\omega_0, \pi/\omega_0)$.

References

- [1] G.C.Carter, *Coherence and Time Delay Estimation: An Applied Tutorial for Research, Development, Test, and Evaluation Engineers*, IEEE Press, 1993.
- [2] C.H.Knapp and G.C.Carter, "The generalized correlation method for estimation of time delay," *IEEE Trans. Acoust., Speech, Signal Processing*, vol.24, no.4, pp.320-327, August 1976.
- [3] J.C.Hassab and R.E.Boucher, "Optimum estimation of time delay by a generalized correlator," *IEEE Trans. Acoust., Speech, Signal Processing*, vol.27, no.4, pp.373-380, August 1979.
- [4] K.Scarbrough, N.Ahmed and G.C.Carter, "On the simulation of a class of time delay estimation algorithms," *IEEE Trans. Acoust., Speech, Signal Processing*, vol.29, no.3, pp.534-540, June 1981.
- [5] X.Ma and C.L.Nikias, "Joint estimation of time delay and frequency delay in impulsive noise using fractional lower order statistics," *IEEE Trans. Signal Processing*, vol.44, no.11, pp.2669-2687, Nov. 1996.
- [6] P.G.Georgiou, P.Tsakalides and C.Kyriakakis, "Alpha-stable modeling of noise and robust time-delay estimation in the presence of impulsive noise," *IEEE Trans. Multimedia*, vol.1, no.3, pp.291-301, Sept. 1999
- [7] C.L.Nikias and R.Pan, "Time delay estimation in unknown Gaussian spatially correlated noise," *IEEE Trans. Acoust., Speech, Signal Processing*, vol.36, no.11, pp.1706-1714, Nov. 1988.
- [8] Y.Wu and A.R.Leyman, "Time delay estimation using higher-order statistics: a set of new results," *Proceedings of 1997 International Conference on Information, Communications and Signal Processing*, vol.3, pp.1397-1400, Singapore, September 1997.

- [9] A.J.Weiss, "Bounds on time-delay estimation for monochromatic signals," *IEEE Trans. Aerospace and Elect. Sys.*, vol.23, no.6, pp.798-808, Nov. 1987.
- [10] S.M.Kay, *Fundamental of Statistical Signal Processing: Estimation Theory*, Englewood Cliffs, NJ: Prentice-Hall, 1993.
- [11] S.M.Kay, *Fundamental of Statistical Signal Processing: Detection Theory*, Upper Saddle River, NJ: Prentice-Hall, 1998.
- [12] A.V.Oppenheim and R.W.Schafer, *Discrete-Time Signal Processing*, Englewood Cliffs, NJ: Prentice-Hall, 1989.
- [13] S.A.Tretter, "Estimating the frequency of a noisy sinusoid by linear regression," *IEEE Trans. Inform. Theory*, vol.31, no.6, pp.832-835, Nov. 1985.
- [14] A.Papoulis *Probability, Random Variables and Stochastic Processes*, McGraw-Hill, New York, 1984.
- [15] D.C.Rife and R.R.Boorstyn, "Single-tone parameter estimation from discrete-time observations," *IEEE Trans. Inform. Theory*, vol.20, no.5, pp.591-598, Sept. 1974.

Figure Captions

Figure 1: Mean square delay errors of a pure sinusoid with known $\omega_0 = 0.345\pi$ for different observation intervals N

Figure 2: Mean square delay errors of a pure sinusoid with known frequency for different ω_0 at $N = 32$

Figure 3: Mean square delay errors of a gated sinusoid with known $\omega_0 = 0.345\pi$ for different rectangular envelopes

Figure 4: Mean square delay errors of a pure sinusoid with unknown $\omega_0 = 0.345\pi$ at $N = 32$

Figure 5: Mean square delay errors of a gated sinusoid with unknown $\omega_0 = 0.345\pi$ for different rectangular envelopes

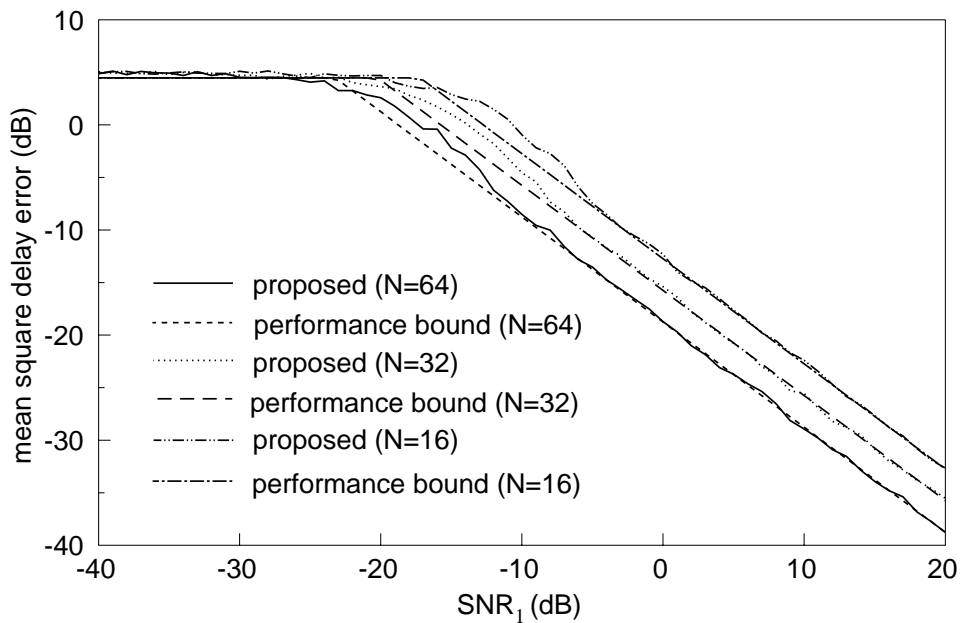


Figure 1:

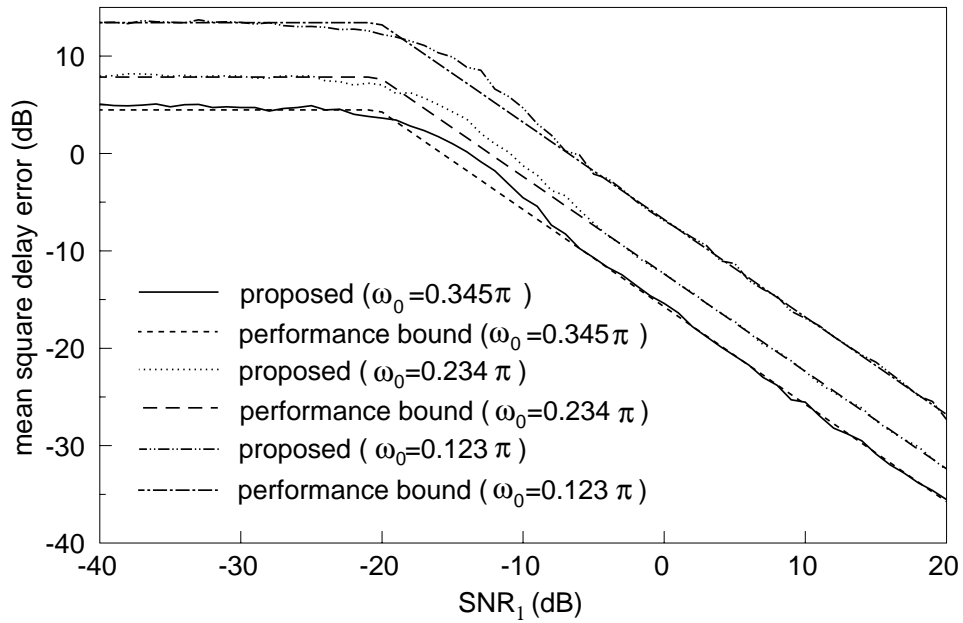


Figure 2:

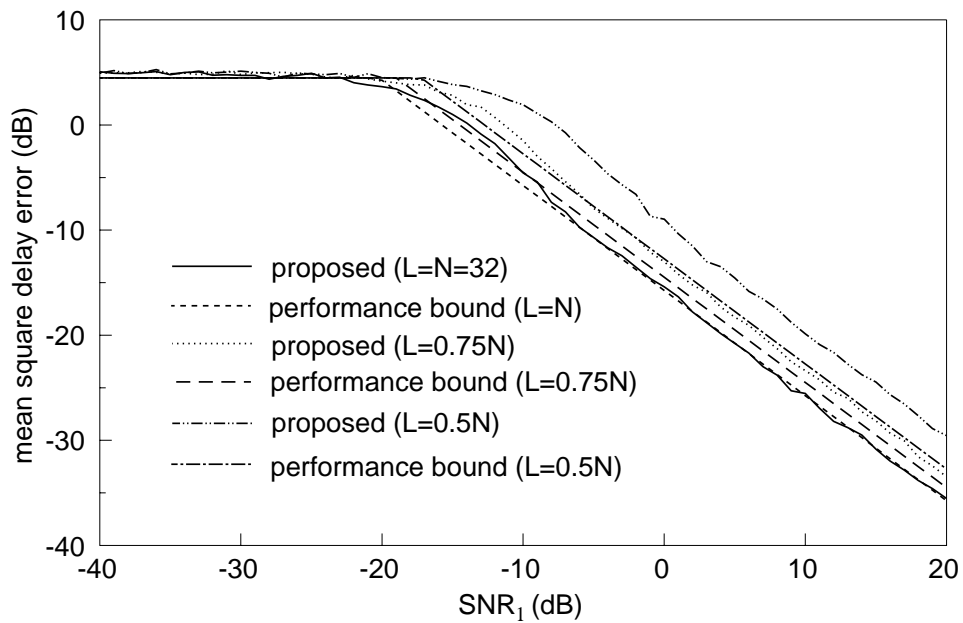


Figure 3:

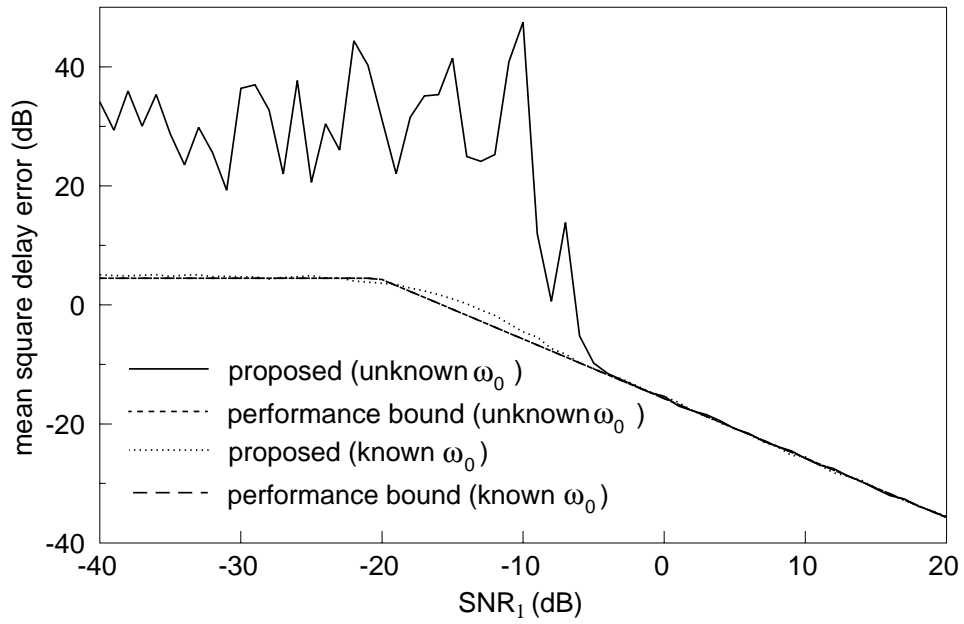


Figure 4:

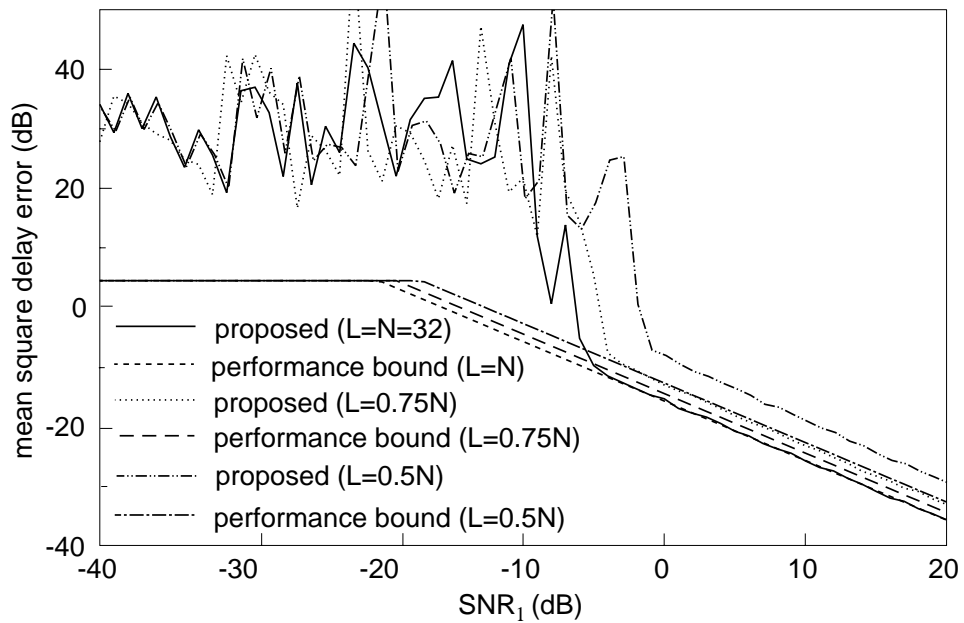


Figure 5: